Ignition of a Ti–Al–C System by an Electron Beam

A. E. Ligachev[a], G. V. Potemkin[b], O. K. Lepakova[c],
M. V. Zhidkov[d,e], A. D. Teresov[b,f], N. N. Golobokov[c],
Yu. M. Maksimov[c], Yu. R. Kolobov[d,e], and N. N. Koval'[b,f]

UDC 541.126

Abstract: This paper describes the optimal modes of initiation of self-propagating high-temperature synthesis with the help of an electron beam on the example of a Ti–Al–C powder mixture. A pulsed electron beam with a particle energy of tens of kiloelectronvolts and a duration of hundreds of microseconds is used. Morphology, structure, and elemental composition of formed products in the form of Ti_3AlC_2 and TiC are studied.

Keywords: high-power pulsed electron beam, self-propagating high-temperature synthesis.

INTRODUCTION

Ignition and subsequent combustion of multicomponent condensed systems is a complex multistep process, which has various physical and chemical stages caused by the existence of zones in various aggregate states, as well as the possibility of chain, sequential, or parallel reactions, unequally significant in different zones [1–3]. It was shown in [3–6] that, in one and the same multicomponent condensed system with the course of competing processes under the same conditions, there could be several stationary combustion wave modes, whose implementation is uniquely determined by the ignition conditions.

The processes of self-propagating high-temperature synthesis (SHS) in M_{n+1}–A–X_n ternary systems, initiated by various heat sources (electric spiral, laser, etc.) are described in sufficient detail in [7, 8].

Considerable scientific and practical interest is given to the ignition of ternary systems by a high-power electron beam and the development of the experimental technique with the stabilization of optimal parameters of the beam for SHS. Accelerators with high-power beams of charged particles are accessible today [9–14] and used to conduct multiple experiments associated with modifying the properties of various materials.

In this paper, the "SOLO" electron-beam device [12] is used to carry out experiments with stimulation of ternary exothermic mixtures by a high-power pulse electron beam in vacuum.

METHODS AND MATERIALS

The experiments are carried out using commercial powders, whose properties are described in Table 1 (D is the fraction size, μ is the molar mass, T_m is the melting point, Q is the latent heat of melting, and K is the number of moles of components calculated for obtaining the compound Ti_3AlC_2, all of which are taken from [15]).

[a]Prokhorov General Physics Institute, Russian Academy of Sciences (GPI RAS), Moscow, 119991 Russia; carbin@yandex.ru.

[b]Tomsk Polytechnic University, Tomsk, 634050 Russia; ep.gvp@yandex.ru

[c]Department of Structural Macrokinetics, Tomsk Scientific Center, Russian Academy of Sciences, Tomsk, 634021 Russia.

[d]Belgorod State University, Belgorod, 308015 Russia.

[e]Institute of Problems of Chemical Physics, Russian Academy of Sciences, Chernogolovka, 142432 Russia.

[f]Institute of High Current Electronics (IHCE), Siberian Branch, Russian Academy of Sciences, Tomsk, 634055 Russia.

Table 1. Characteristics of the powders used

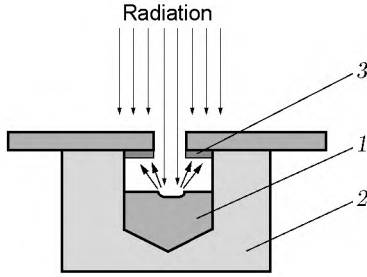| Element	Powder type	D, μm	μ, g/mol	T_m, °C	Q, kJ/mol	K
Ti	PTS	≈150	48	1668	15.5	3
Al	ASD-4	10–50	27	660	10.8	1.1
C	PM15	0.3–0.5	12	4500	—	1.8

Fig. 1. Experimental diagram for the irradiation of Ti–Al–C system: (*1*) Ti–Al–C powder mixture pellet; (*2*) graphite crucible; (*3*) aperture.

Figure 1 shows the experimental diagram for the synthesis of the SHS products using an electron beam. A Ti–Al–C powder mixture pellet (15 mm in diameter, 10 mm in thickness, 5 g in mass, and with 40% of porosity) are placed in a graphite crucible 20 mm in height with a blind hole 15 mm in diameter and covered by a copper diaphragm with a ≈5-mm hole for the passage of an electron beam into the crucible. The crucible is placed in a vacuum chamber with an electronic source with a plasma cathode.

An electron beam is used with the energy $E_0 = 15$ keV, pulse duration $\tau = 200$ μs, repetition rate of 1 Hz, and practically uniform distribution of the density flux along the cross section of the beam, whose dimensions on the pellet with an area of 0.2 cm^2 are determined by the input diaphragm (see Fig. 1). The energy density measured by the calorimeter at the entrance to the crucible is ≈ 40 J/cm^2 with the heat flux in the spot on the pellet is equal to $\approx 2 \cdot 10^5$ W/cm^2.

The weight of the samples before and after treatment is measured on an LV-210-A analytical scale.

The structure and elemental composition of the treated samples are studied on a FEI Quanta 600 electron microscope. The phase composition of the materials obtained is determined on a DRON-2 diffractometer with Co K_α radiation in the Bragg–Brentano focus mode.

EXPERIMENTAL RESULTS AND DISCUSSION

Gas- and hydrodynamic processes and chemical transformations occurring at the stage of ignition can be understood if there is a clear idea of the space–time pattern of the interaction of the high-power electron flux with the Ti–Al–C porous heterogeneous system characterized by varying dispersiveness of the components.

The energy is pumped by an electron beam through the electron subsystem of an irradiated body, and the energy exchange with the phonon subsystem occurs through a characteristic time equal to the relaxation period: $\tau_{ei} \approx \tau_0 = 10^{-10}$ s [16–18]. For electrons with the energy $E_0 \leqslant 300$ keV, the main mechanism of electron absorption is the Coulomb scattering. At the same time, two-thirds of the beam energy goes to the excitation of bound electrons and the rest to ionization.

If the inflow rate of the energy (in W/cm^2) is comparable or larger with respect to the heat sink rate, the metal melts and subsequently evaporates due to the thermal conductivity in a solid in the energy release zone. The depth of the energy release zone is determined by the mean free path R of the electron of the given energy in a particular substance (Ti, Al, C, and gas). The dimensions of the energy release zone can be estimated by using the Kanaya–Okayama equation [19]

$$R = 2.76 \cdot 10^{-2} \mu E_0^{1.67}/Z^{0.89} \rho \ [\mu\text{m}], \qquad (1)$$

where ρ [g/cm^3] is the density of the irradiated substance, and Z is the atomic number. Table 2 illustrates the values of Z along with the values of the thermal diffusivity of the irradiated materials a_i, of the binding energy of the elements ε [16], and of the threshold flux densities q_c, for which the materials fracture (evaporation and removal in a liquid phase) [18, 20]. The study of the dynamics of the interaction of high-current electron beam with transparent low-density aerogel by optical methods showed that the size of the bulk energy release zone corresponds to the free path of electrons of a given energy in a particular substance and remains unchanged with constant parameters of the electron beam [14].

Table 2. Thermophysical parameters of the mixture elements

Element	Z	ε, eV/atom	ρ, g/cm^3	R, μm	q_c, W/cm^2	ΔH, kJ/kg	a, m^2/s
C	6	7.36	3.5	3.5	—	59	$1.22 \cdot 10^{-3}$
Al	13	3.34	2.7	2.8	$2 \cdot 10^5$	10.8	$8.42 \cdot 10^{-5}$
Ti	22	4.86	4.5	1.4	—	9.8	$8.30 \cdot 10^{-6}$

The sizes of the Al and Ti fractions (see Table 1) are larger than the free paths R of the electrons with the energy $E_0 = 15$ keV (see Table 2) by more than an order of magnitude, and the diameters of soot (carbon) particles are an order of magnitude smaller than the free path R_C. The initial surface of the Ti–Al–C pellet, on which the beam falls, has the Ti, Al, and C elements distributed mosaically thereon, and the irradiated heterogeneous body is a mixture of particles with varying dispersity and orientation. Assuming that the pellet pores containing CO, H_2, O_2 and N_2 [21] are the same in size with the carbon fraction, we can calculate the effective thermal diffusivity of the mixture ($a \approx 0.5a_{Ti} + 0.31a_C + 0.19a_{Al}$) with a given porosity of 40% [22] and determine the size of the thermal effect zone (L_h) in condensed matter under the action of the electron beam with given parameters. The layer of the heated heterogeneous substance (thermal effect zones) increases for the radiation time τ in accordance with the equation

$$L_h = \sqrt{a\tau} \tag{2}$$

[17, 18, 20]. If the energy of the electron beam equals to tens of kiloelectronvolts and the density created by the electron beam is $q_0 \geqslant 10^4$ W/cm^2, the processes of evaporation and fracture of the surface of the processed material become essentially important [18, 20, 23].

The total thermal balance of the thermal effect zone in this case can be estimated in the expression

$$Q_e + Q_r = Q_s + Q_f + Q_v, \tag{3}$$

where Q_e is the energy introduced by the electron beam, Q_r is the thermal effect of exothermic reactions, Q_s is the heat flux caused by the thermal conductivity mechanism, and Q_f and Q_v are the heats of melting and evaporation, respectively.

If, during the irradiation time, the layer of the material L_h obtains the energy comparable to the specific heat of evaporation, the evaporation process becomes governing [23]:

$$q_{cr} \sim \Delta H \rho L_h. \tag{4}$$

This condition for the electron beam with a critical heat flux (specific density) $q_{cr} \approx q_0 \approx 2 \cdot 10^5$ W/cm^2 is satisfied. In the absorbing layer of the Ti–Al–C pellet, there is the phase transition of a condensed substance into a
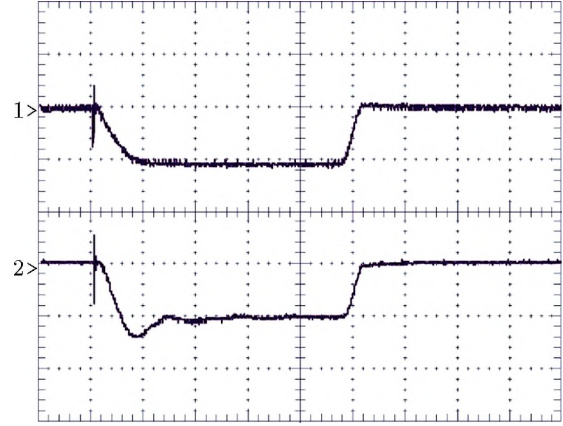

Fig. 2. Current oscillograms of the "SOLO" device [10]: (1) discharge current I_d; (2) electron beam current I_g; the abscissa axis is 50 μs/div, and the ordinate axis is relative units per division.

gaseous one, and the heat conduction mechanism determines the temperature distribution in the condensed phase only behind the moving boundary of evaporation [18, 20]. If $Q_s \gg Q_r$ in the layer, there is no stable combustion of the mixture and no combustion wave. The temperature profile of the combustion wave becomes observable only in the region where $Q_s < Q_r$.

In this experiment, the effect of a single electron pulse (Fig. 2) on the pellet of the ternary mixture ends with a bright flash (optical radiation is recorded with a high-speed camera) and a pressure jump in the accelerator chamber.

The melting process followed by evaporation is triggered by the leading edge of the pulse radiation. The trailing edge of the pulse $\approx$10 μs (see Fig. 2), in turn, triggers the high-rate solidification process.

The cylindrical pellet turns into a thick-walled shell after being treated with an electron beam, which is illustrated in Fig. 3. Explosion-like phase transitions in the exothermic porous system under the action of a high-power electron beam lead to the removal of the substance from the sample, reaching 60% of the initial mass, to the formation of regions with different surface topographies, and to an increase in the volume of the condensed object by approximately 2.5 times.
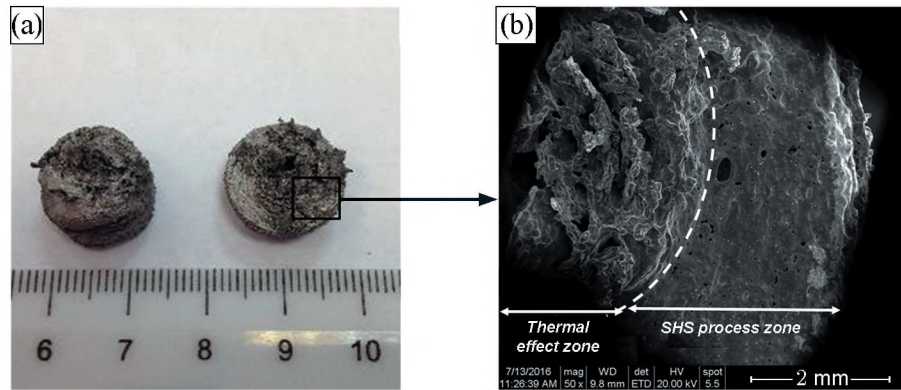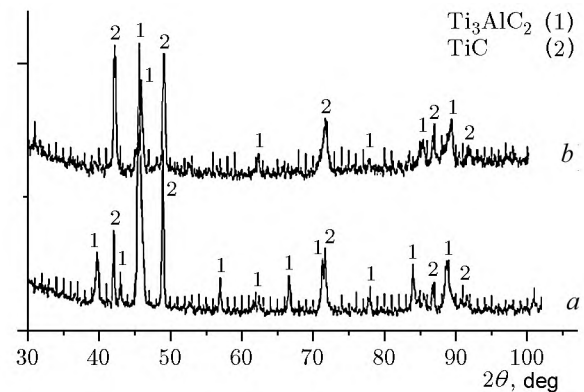
Fig. 3. General view (a) and structure (b) of the Ti–Al–C samples after treatment by a high-power electron beam.

**Fig. 4.** Frontal view of the bottom part of the treated pellet.

Fig. 5. Diffractograms of the SHS products: ignition of the mixture by electromagnetic radiation in an argon medium at a pressure of 5 atm (curve a) and ignition of the mixture by a high-power electron beam in vacuum (curve b).

To study the structure and elemental composition of the formed substance, the sample is cut approximately along the boundary between the top foamed part (gel) and bottom part [SHS product (dashed curve in Fig. 3b)].

The top part of the sample is significantly different from the bottom one (Fig. 4), which looks like a standard SHS product. There is a through hole with an incorrect shape, which is a canal formed by the shock-wave effect of the electron beam. The effect of the beam lead to dagger penetration, almost complete removal from the top part of the aluminum sample, and partial removal of titanium and carbon. The removal of the substance matter from the sample volume is associated with high-rate evaporation and formation of CN, C_2N_2,

C_4N_2, CO, and CO_2 gases. The density of the formed product in the top part of the sample (see Fig. 3b) is noticeably smaller than in the bottom one (see Fig. 4).

The specific energy released during the time of the radiation pulse in the energy release zone ($\approx R_c$), exceeds the binding energy of atoms in the elements by several orders of magnitude (see Table 2) [16, 24], so the energy input of the chemical reactions in this zone is insignificant. The ignition of the SHS process itself in the strongly nonequilibrium Ti–Al–C system occurs outside the thermal effect zone ($L_h \approx 0.5$ mm) (see the bottom part in Fig. 3 and cylinder walls in Fig. 4).

The power in the spot on the pellet produced by the high-power electron beam and equal to $q_0 \approx 2 \times 10^5$ W/cm^2 exceeds the standard one [2, 25] $q = (1–2) \cdot 10^2$ W/cm^2 by three orders of magnitude and indicates that the ignition occurs in the region of the right branch
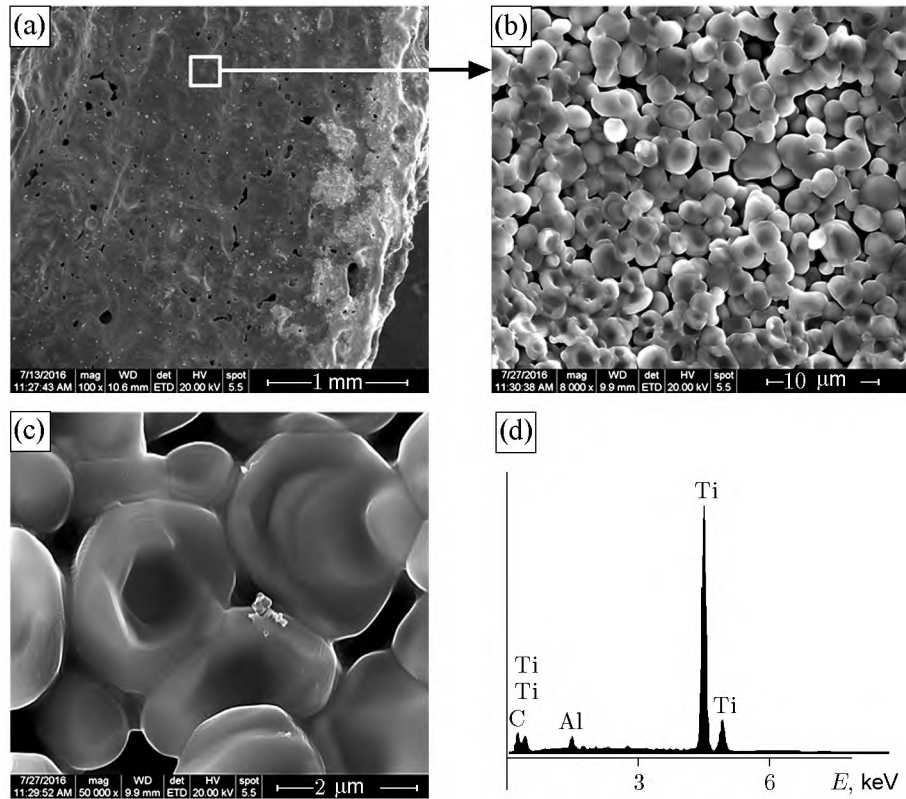
Fig. 6. Structure of the peripheral region (SHS process zones) of the Ti–Al–C sample after treatment with an electron beam: (b, c) morphological features of TiC crystals at different zooms; (d): 26.64% CK, 3.84% AlK, and 69.52% TiK.

of the curve illustrating the igniting pulse versus the density of the heat flux [24], when the temperature at the boundary of the phase transition reaches a value close to a boiling point of the material T_b [18, 20, 25]. The duration of the ignition delay determined by the video recording is ≈ 0.1 s, the duration of the bright flash (SHS process) is equal to ≈ 4 s, and the duration of the glow of the cooling SHS product is 10–12 s.

With high-speed energy supply to the irradiated target, compression and rarefaction waves are formed therein. The appearance of a rarefaction wave can also lead to the release of substance from the irradiated target in a direction opposite to the direction of the electron beam [13, 14, 26].

The diffractograms of the SHS products illustrated in Fig. 5 with the use of various ignition methods show different ratios of Ti_3AlC_2 and TiC. According to the data of the quantitative x-ray phase analysis, the sample a contains $\approx 75\%$ of Ti_3AlC_2 and 25% of TiC and the sample b treated by the electron beam contains 18% of Ti_3AlC_2 and 82% of TiC. Such a difference in the phase ratio can be explained by the conditions for the SHS initiation of in these samples.

The composition of the substance in the top part of the sample treated with the electron beam (see Fig. 5) does not show the x-ray amorphous fraction of the product in the form of amorphous Ti and ultrafine phases of other compounds [27], which are present in the solidification of the melt with a temperature gradient of 10^6 K/cm and velocities of the interface boundaries of the order of 1 m/s [28].

In the case of irradiation by a high-power electron beam, the TiC phase predominates due to the intense evaporation of the low-melting component of Al. When the thermal energy of atoms of the irradiated material, obtained from the high-power electronic beam, decreases to a value comparable to the energy of interacting particles in the exothermic reaction, the SHS process begins in the target. Spatially, it is realized outside the thermal effect zone, and titanium carbide identified in this zone is not a product of SHS. In the temporary scale radiation, the TiC synthesis occurs after the end of the pulse (a few milliseconds). Nanolaminates are the products of the SHS process and formed at the periphery of the sample, where part of aluminum is still retained, not evaporated, and not removed in the liq-

uid phase under the action of the high-power electron beam.

With high-rate solidification of the metallocarbon melt, the resulting structure of titanium carbide with Ti_3AlC_2 inclusions is a low-density gel-like product. The microstructures shown in Figs. 6a–6c characterize the morphological features of the cylindrical surface of the shell (see Fig. 4). The data of the energy dispersion analysis (Fig. 6d) show that, in this region, there is almost no aluminum, and the structural elements are mainly represented by titanium carbide in the form of hollow hemispheres (Figs. 6b and 6c).

The complete picture of the processes occurring in exothermic ternary porous mixtures under the action of high-power electron beams is far from clear and needs further research.

CONCLUSIONS

Under the action of the high-power electron beam, the Ti–Al–C sample radically changes its shape and content—the pellet turns into an inverted shell with a bulging bottom.

Under the action of the electron beams with a power density of more than 10^3 W/cm^2, there is a change in the elemental composition due to removal of low-melting components from the mixture.

The use of high-power electron beams is effective for obtaining spatially heterogeneous structures, different by porosity and phase composition in depth.

REFERENCES

1. A. G. Strunina, V. I. Ermakov, S. V. Kostin, et al., "Choice of Optimal Ignition Conditions for Hard-to-Ignite Gasless Systems," Fiz. Goreniya Vzryva **17** (4), 3–9 (1981) [Combust., Expl., Shock Waves **17** (4), 351–356 (1981)].
2. V. P. Stovbun, T. I. Kedrova, and V. V. Barzykin, "Ignition of Systems with High-Melting Reaction Products," Fiz. Goreniya Vzryva **8** (3), 349–354 (1972) [Combust., Expl., Shock Waves **8** (3), 279–283 (1972)].
3. *Concepts of Development of SHS as a Field of Scientific and Technological Progress*, Ed. by A. G. Merzhanov (Territoriya, Chernogolovka, 2003) [in Russian].
4. T. P. Ivleva, A. G. Merzhanov, and K. G. Shkadinskii, "A New Type of Nonuniqueness of Stationary Modes of the Combustion Wave Propagation," Dokl. Akad. Nauk SSSR **256** (4), 897–884 (1981).
5. E. A. Levashov, Yu. V. Bogatov, and A. A. Milovidov, "Macrokinetics and Mechanism of the SVS-Process in Systems on a Titanium–Carbon Base," Fiz. Goreniya Vzryva **27** (1), 88–93 (1991) [Combust., Expl., Shock Waves **27** (1), 83–88 (1991)].
6. V. N. Vilyunov, *Theory of Ignition of Condensed Matter* (Nauka, Novosibirsk, 1984) [in Russian].
7. M. W. Barsoum and T. El-Raghy, "The MAX Phases: Unique New Carbide and Nitride Materials," Amer. Sci. **89** 334–343 (2001).
8. E. A. Levashov, Yu. S. Pogozhev, D. V. Shtanskii, et al., "Self-Propagating High-Temperature Synthesis of Ceramic Materials on the Basis of $M_{n+1}AX_n$ in the Ti–Cr–Al–C System," Izv. Vyssh. Uchebn. Zaved., Poroshk. Metallurg. Funkts. Pokr. **3** 13 (2008).
9. A. V. Khaneft, "Criteria for Igniting Condensed Substances by an Electron Pulse," Khim. Fiz. **17** (8), 132 (1998).
10. B. P. Aduev, G. M. Belokurov, S. S. Grechin, et al., " Detonation of PETN Single Crystals Initiated by an Electron Beam," Fiz. Goreniya Vzryva **46** (6), 111–118 (2010) [Combust., Expl., Shock Waves **46** (6), 712–718 (2010)].
11. V. I. Korepanov, V. M. Lisitsyn, V. I. Oleshko, et al., "PETN Detonation Initiated by a High-Power Electron Beam," Technical Physics Letters **29** (8) [Pis'ma Zh. Tekh. Fiz. **29** (16), 23–28 (2003)].
12. S. V. Grigoriev, V. N. Devjatkov, N. N. Koval, et al., "The Automated Installation for Surface Modification of Metal and Ceramic–Metal Materials and Products by an Intensive Pulse Sub-Millisecond Electron Beam," in *Proc. 9th Int. Conf. Modification of Materials with Particle Beams and Plasma Flows* (Tomsk, Russia, 21–26 September 2008).
13. V. A. Artemov, M. A. Vlasov, O. A. Malafeev, et al., "Experimental Study of Nonstationary Evaporation of Metal Under the Action of an Electron Beam," Zh. Tekh. Fiz. **48** (2), 192–195 (1978).
14. B. A. Demidov, V. P. Efremov, M. P. Ivkin, et al., "Determination of the Energy Release Profile in Aerogel," Zh. Tekh. Fiz. **67** (11), 26 (1997).
15. Y. Zou, Z. M. Sun, H. Hashimoto, et al., "Low Temperature Synthesis of Single-Phase Ti_3AlC_2 through Reactive Sintering Ti/Al/C Powders," Mater. Sci. Eng. A **473**, 90–95 (2008).
16. C. Kittel, *Introduction to Solid State Physics* (Wiley, 1956).
17. A.V. Lykov and B. M. Smolskii, *Heat and Mass Transfer* (Energiya, Moscow, 1972; Jerusalem, Israel, 1967).
18. F. F. Vodovatov, A. A. Chel'nyi, V. P. Veiko, et al., *Lasers in Technology* (Energiya, Moscow, 1975) [in Russian].

19. K. Kanaya and S. Okayama, "Penetration and Energy Loss Theory of Electrons in Solid Targets," J. Phys., D. Appl. Phys. **5**, 43–58 (1972).

20. N. N. Rykalin, A. A. Uglov, I. V. Zuev, *Fundamentals of Electron-Beam Treatment of Materials* (Mashinostroenie, Moscow, 1978) [in Russian].

21. V. F. Brekhovskikh, N. N. Rykalin, and A. A. Uglov, "On the Possible Effect of Gas Content in Metals on the Area Affect by a Laser Beam," Dokl. Akad. Nauk SSSR **190** (5), 1059 (1970).

22. A. Missenard, *Conductivite Thermique des Solides, Liquides, Gaz et de Leurs Melanges* (Editions Eyrolles, 1965).

23. Yu. V. Afanas'ev and O. N. Krokhin, *Vaporization of Matter Exposed to Laser Emission* (Zhurn. Eksp. Teoret. Fiz. **52** 966–975 (1967) [J. Exptl. Theret. Phys. **52** 639–645 (1967).

24. A. A. Koval'skii, S. S. Khlevnoi, V. F. Mikheev, "The Ignition of Ballistite Powders," Fiz. Goreniya Vzryva **3** (4), 527–541 (1967) [Combust., Expl., Shock Waves **3** (4), 323–331 (1967)].

25. L. G. Strakovskii, P. I. Ulyakov, E. I. Frolov, " Role of Vaporization in Explosive Ignition," Fiz. Goreniya Vzryva **16** (6), 59–64 (1980) [Combust., Expl., Shock Waves **16** (6), 654–659 (1980)].

26. G. I. Kanel, S. V. Razorenov, A. V. Utkin, et al., *Shock-Wave Phenomena in Condensed Media* (Yanus-K, Moscow, 1996) [in Russian].

27. G. Nicolis and I. Prigogine, *Self-Organization in Nonequilibrium Systems: From Dissipative Structures to Order Through Fluctuations* (Wiley, 1977).

28. W. Kurz and D. J. Fisher, *Fundamental of Solidification* (Trans Tech Publications, 1986).